Physics – Uspekhi **62** (2) 186 – 197 (2019)

METHODOLOGICAL NOTES PACS numbers: **03.65. – w**, **31.10. + z**, 31.15.bt

Semiclassical method of analysis and estimation of the orbital binding energies in many-electron atoms and ions

G V Shpatakovskaya

DOI: https://doi.org/10.3367/UFNe.2018.02.038289

Contents

Abstract. Orbital binding energies in the ground state of many-electron elements obtained in experiments or in quantum-mechanical calculations are studied. Their dependences on the atomic number and on the degree of ionization are analyzed. The Bohr – Sommerfeld semiclassical quantization condition is used and filled-shell orbital binding energy approximate scaling is shown. The scaling is similar to the one in the Thomas – Fermi model, but with two other functions-coefficients. The effective method of the demonstration of binding energies in a large number of atoms through these two functions is proposed. As a result, special features of the elements of the main and transition groups and the influence of relativistic effects are vividly manifested. Simple interpolation expressions are built for the two functions. One can use them to estimate orbital binding energies in the filled shells of many-electron atoms and ions to within 10% for middle elements and from 10% to 30% for heavy ones. The estimate can be used as the initial approximation in precessional atomic computations and also for rough calculations of the ionization cross sections of many-electron atoms and ions by electrons and heavy particles, failing more precise data.

Keywords: periodic system, semiclassical approximation, electron binding energy, atomic number scaling, ionization state, orbital angular momentum

G V Shpatakovskaya Keldysh Institute of Applied Mathematics, Russian Academy of Sciences, Miusskaya pl. 4, 125047 Moscow, Russian Federation. E-mail: shpagalya@yandex.ru

Received 18 October 2017, revised 20 January 2018
Uspekhi Fizicheskikh Nauk **189** (2) 195 – 206 (2019)
DOI: https://doi.org/10.3367/UFNr.2018.02.038289
Translated by Yu V Morozov; edited by A Radzig

1. Introduction

Mendeleev's Periodic Table of elements is known to place atoms in order of ascending atomic number (nuclear charge Z) [1] and arrange them in periods in accordance with the electron shell configuration of an atom, each period ending with an inert gas. Therefore, the electron configuration of elements in each next period is often represented, for brevity, as the symbol of the inert gas followed by the description of the structure of the electron shells filled in this element, e.g., the electron configuration of nickel can be specified as [Ar] $3d^8 4s^2$, and that of cadmium as [Kr] $5s^2$. Also, elements are distinguished by their belonging to the main or transition groups; in the latter, d- and f-states are filled. These 'school' information raises the following questions: 'What do these features reflect in quantitative values of electron binding energies and other atomic characteristics?' 'How do electron binding energies in atoms and ions depend on the atomic number and ion charge?' 'What is this dependence like in the elements of the main groups and how does it differ from the dependence in the elements of the transition groups?' 'What can the influence of relativistic effects lead to?'

The present study was designed in an attempt to answer these questions based on the statistical Thomas–Fermi (TF) model [2–4], i.e., a quasiclassical approximation in the framework of the nonrelativistic self-consistent field model, as the starting point. The TF model was and is not infrequently used to estimate atom and ion characteristics [5–8], despite its low accuracy compared with that of quantum-mechanical calculations [9–14] taking account of relativistic effects.

In our approach [15–17], the TF model is exemplified as a tool in the search for atomic number and degree of ionization scaling by means of successive analysis of experimental and

theoretical orbital binding energies in many-electron atomic systems.

The source of experimental data on atomic energy levels of elements from hydrogen to uranium was data booklet [18], summarizing material from Refs [19–22] for atoms. Results of calculations for atoms and ions by density functional [11, 13, 23] and self-consistent field [9, 10, 12, 24] methods served as theoretical data. It should be here noted the lack of literature information on the characteristics of heavy element ions needed for both experimental studies and basic research.

The paper layout is as follows. Section 2 is devoted to the behavior of the intraatomic potential in atomic systems. Experimental and theoretical binding energies of s-electrons in atoms are considered in Section 3 and calculated binding energies in ions in Section 4. Section 5 presents the quasiclassical analysis of the dependences of binding energies on the orbital angular momentum in atomic potentials. Section 6 concerns research on experimental and theoretical binding energies of electrons with nonzero orbital angular momenta with regard to and regardless of relativistic effects in atoms. Calculated data for ions of middle and heavy elements are discussed in Sections 7.1 and 7.2, respectively.

2. Intraatomic potential

First, we consider the spherically symmetric variant of the TF model most suitable for the description of many-electron atomic systems (atoms and positive ions) with filled shells. In the case of atoms, it relates to inert gases with atomic numbers $Z \gg 1$, and in the case of ions to the systems with a number of electrons $N_e \gg 1$. How much greater than unity these values should be is clear from the concrete examples below comparing results obtained in the framework of the TF model and quantum-mechanical models for inert gases.

In the TF model of a free ion with charge z, the electron potential energy $U_{TF}(r)$ in an atom with atomic number Z is given by the function $\varphi_{TF}(x;\alpha)$ — the solution of the TF equation [1]:

$$U_{TF}(r;z,Z) = -\frac{Z\varphi_{TF}(x;\alpha)}{r}\,, \quad \alpha = \frac{z}{Z}\,, \qquad r = c\,xZ^{-1/3}\,, \quad c = 0.88534\,; \tag{1}$$

$$\sqrt{x}\,\varphi''_{TF} = \varphi_{TF}^{3/2}\,, \quad \varphi_{TF}(0;\alpha) = 1\,, \quad x_0\varphi'_{TF}(x_0;\alpha) = -\alpha\,. \tag{2}$$

Hereinafter, Hartree atomic units are used unless otherwise specified. At $\alpha = 0$, one has $x_0 = \infty$ and equation (2) describes the potential in a neutral atom. Function $\varphi_{TF}(cx;0)$ for an atom is plotted as a curve in Fig. 1.

These relations show that there is an atomic number and the degree of ionization scaling of interatomic potential in a very simple TF model disregarding many important physical effects (exchange, gradient, relativistic, etc.). A valid question: Is there such a scaling, even if approximate, of the potential calculated based on more advanced quantum-mechanical models?

To answer this question in the case of neutral atoms, intraatomic potentials of five inert gases (neon, argon, krypton, xenon, and radon) were calculated from the modified Hartree–Fock–Slater (MHFS) model [12] and by the density functional method with scalar relativistic corrections using program [13]. The two approaches yielded very similar results in the inner atomic regions of interest, while differences at the periphery were due to taking account of the self-action effect in the MHFS model.

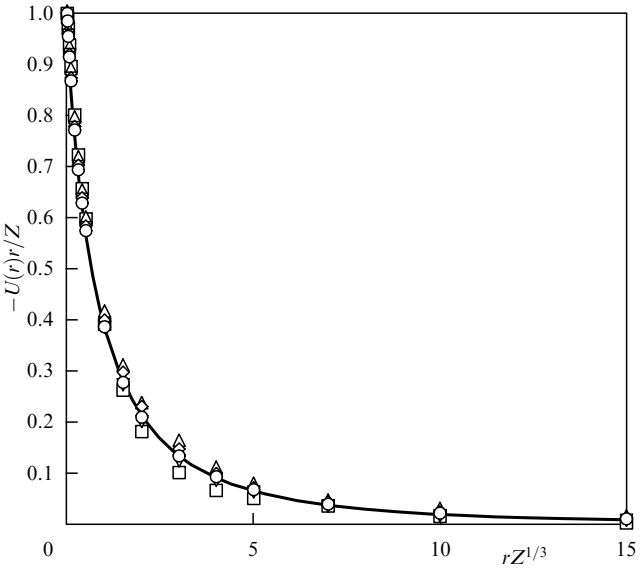

Figure 1. Dependence of reduced intraatomic potential $-U(r)r/Z$ on reduced radius $rZ^{1/3}$ in the TF model (curve) and model [13] for inert gases (symbols): neon ($Z = 10$) — □, argon ($Z = 18$) — △, krypton ($Z = 36$) — ▽, xenon ($Z = 54$) — ◇, and radon ($Z = 86$) — ○.

Figure 1 presents, in addition to the TF function, the results of calculations by the density functional method [13] for inert gas atoms (symbols). The figure shows that the results are close to the respective function in the TF model, especially for many-electron atoms with $Z \geqslant 18$. This means that for the intraatomic potential of such inert gases the atomic number scaling in the following form is approximately true:

$$-U(r) = \frac{Z\varphi(rZ^{1/3})}{r}\,, \tag{3}$$

where the function $\lg\varphi(x)$ in the $0 \leqslant x \leqslant 15$ range can be interpolated employing the cubic polynomial:

$$\lg\varphi(x) = \sum_{k=0}^{3} f_k x^k\,, \quad f_0 = -0.03379\,,$$
$$f_1 = -0.34948\,, \quad f_2 = 0.02880\,, \quad f_3 = -0.00093\,.$$

As is shown below, the scaling of potential leads to the atomic number scaling of energy levels in this potential, first and foremost for s-electrons.

3. Binding energies of s-electrons in atoms

3.1 Thomas–Fermi model

Let us consider energy levels in an atom with the atomic number Z in the framework of the TF model (1), (2). The nonrelativistic energy levels E_{nl} in the central potential depend on two quantum numbers: the principal n and orbital l ones; in the quasiclassical approximation, they can be determined from the Bohr–Sommerfeld quantization condition. In the case of s-states ($l = 0$), it has the form

$$S_E = \int_0^{R_E} \sqrt{2\big[E - U(r)\big]}\,\mathrm{d}r = \pi n\,. \tag{4}$$

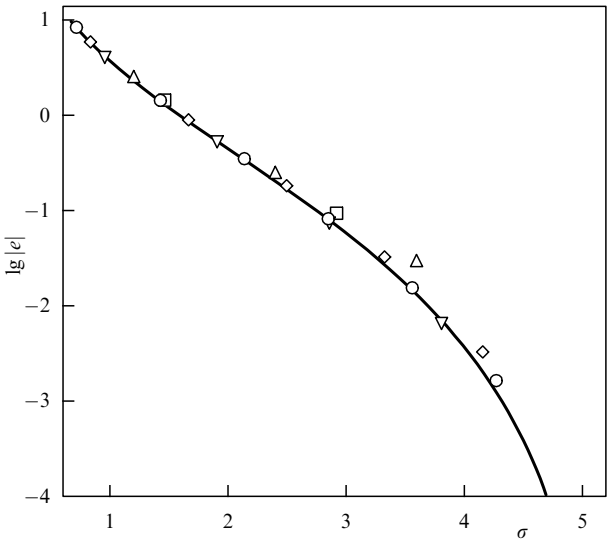

Figure 2. Dependences of reduced energies $e_n = E_{n0}/Z^{4/3}$ of s-electrons on the reduced action $\sigma_n = \pi n Z^{-1/3}$ obtained using the TF model (curve) and deduced from calculations for inert gas atoms [23] based on non-relativistic LDA model [11] (symbols: notations are the same as in Fig. 1).

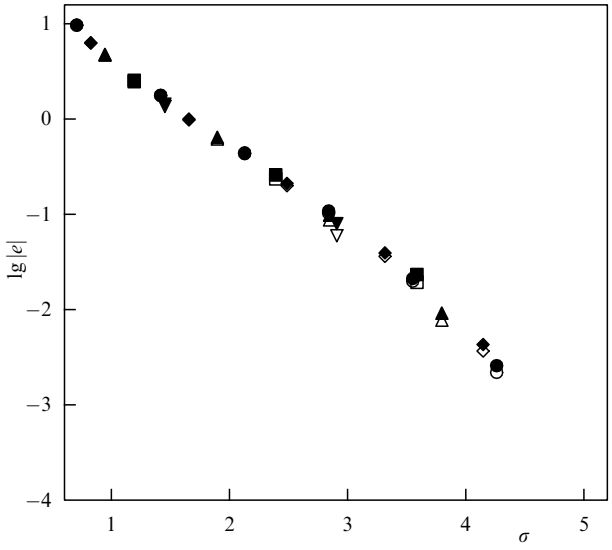

Figure 3. The same as in Fig. 2 for inert gases in the scalar relativistic model ScRLDA [11, 23] (unfilled symbols) and based on experimental data [18] (filled symbols). See Fig. 1 for notations.

Here, S_E is the action of an electron with energy E and zero orbital angular momentum, $U(r)$ is the electron potential energy, and the region of integration is bounded by the turning point R_E.

Introducing the notation

$$E_{n0} = Z^{4/3} e_n \tag{5}$$

and substituting TF potential (1) for the atom ($\alpha = 0$) into formula (4) yield explicitly Z-dependences:

$$\begin{aligned} &S_E = Z^{1/3}\sigma(e) = \pi n\,, \\ &\sigma(e) = \sqrt{2c}\int_0^{X_e} \sqrt{\frac{\varphi_{TF}(x)}{x} + ce}\ \mathrm{d}x\,. \end{aligned} \tag{6}$$

Here, quantities σ and e correspond to the s-electron action and energy for $Z = 1$, and $X_e = R_E Z^{1/3}/c$. In the general case, smaller values of $\sigma_n = \pi n Z^{-1/3}$ correspond to the inner filled shells and heavier atoms, while larger values relate to the outer shells being filled and lighter atoms.

Expression (6) assigns e_n to each σ_n value and thereby establishes the functional dependence $e(\sigma)$ in the TF model, depicted by the curve in Fig. 2 on the semilogarithmic scale. Notice a wide range of function $e(\sigma)$ variation (over a few orders of magnitude upon a change in σ by several units) responsible for the logarithmic accuracy of all apparent coincidences and proximity of values referred to below.

3.2 Atoms of inert gases

The symbols in Fig. 2 denote reduced energies of all s-electrons in the atoms of five inert gases calculated by the nonrelativistic LDA model [11] and borrowed from tables [23] [1].

To obtain the required data, s-state energies E_{n0} were taken from the tables [23] and the value of $\sigma_n = \pi n Z^{-1/3}$ was assigned to

$$e_n = \frac{E_{n0}}{Z^{4/3}}\,.$$

Figure 2 confirms the existence of the approximate common dependence $e(\sigma)$ for many-electron inert gases close to the one calculated from the TF model.

Figure 3 shows an analogous dependence for inert gas atoms in the respective experimental data [18] and the results obtained by the density functional method, taking account of scalar relativistic effects (ScRLDA) [23]. The differences between the energies of s-electrons in Figs 2 and 3 are due to relativistic effects most pronounced in heavy elements. They have an especially strong impact on the binding energies of electrons with nonzero orbital angular momentum (see Section 6).

The dependence $\lg|e(\sigma)|$ for experimental data in Fig. 3 can be approximately interpolated using the cubic polynomial

$$\begin{aligned} &\lg\left|e(\sigma)\right| = \sum_{k=0}^{3} a_k \sigma^k\,, \quad a_0 = 1.92027\,, \\ &a_1 = -1.59497\,, \quad a_2 = 0.35069\,, \quad a_3 = -0.05253\,. \end{aligned} \tag{7}$$

This interpolation obtained from the data for inert gases will be used below to estimate electron binding energies in atoms of other elements.

3.3 Atoms of Periodic Table of elements from neon to uranium

Tables [23] and [18] [2] provide copious material for investigations into consistent patterns of all atoms from hydrogen to uranium.

[1] Tables [23] contain information on electron binding energies E_{nl} in the ground state of atoms and first ions from hydrogen to uranium, calculated by several versions of density functional method [11] with and without regard for relativistic effects.

[2] Reference [18] reports binding energies measured in the natural state of elements. Therefore, it lacks some upper levels of free elements (unlike calculated results [23]).

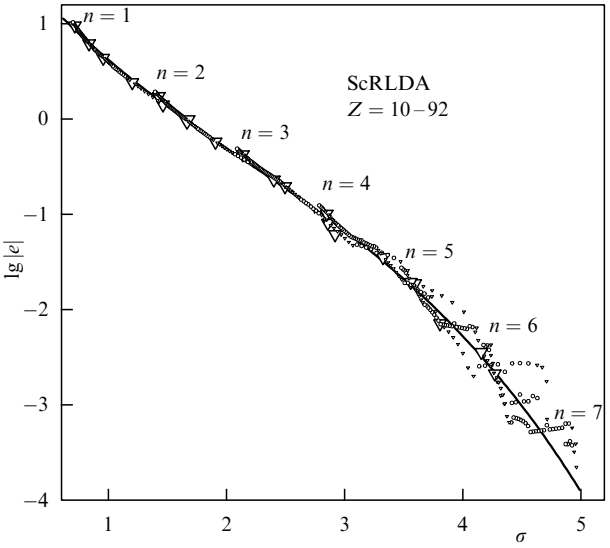

Figure 4. Dependence $\lg|e(\sigma)|$ for all elements from neon ($Z = 10$) to uranium ($Z = 92$). Graphical interpretation of the binding energies calculated by ScRLDA model [23]: ▽ is the main group elements (large ▽ symbols mark inert gases), ○ is the transition group elements. The curve is the interpolating cubic polynomial for inert gases.

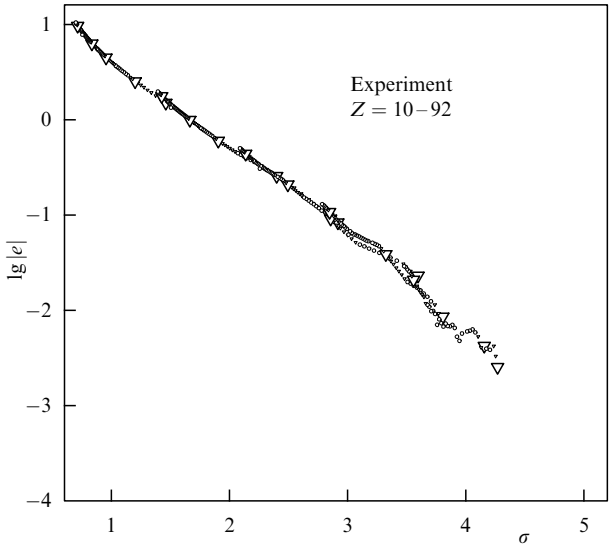

Figure 5. Dependence $\lg|e(\sigma)|$ for all elements from neon ($Z = 10$) to uranium ($Z = 92$). Graphical interpretation of experimental binding energies [18]: ▽ is the main group elements (large ▽ symbols mark inert gases), ○ is the transition group elements.

ScRLDA (scalar relativistic model) data and the observed binding energies processing results are illustrated in Figs 4 and 5. Two different symbols (▽ and ○) denote elements of the main and transition groups; bigger symbols ▽ mark inert gases. The interpolation cubic polynomial for five inert gases is represented by the curve in Fig. 4. In addition, the sites where a shell with the new principal quantum number n appears are indicated.

Figures 4, 5 demonstrate the possibility to simultaneously overview voluminous information on electron s-state energies for the 83 atoms using the function $\lg|e(\sigma)|$. Evidently, the values of $\lg|e(\sigma)|$ for all atoms are very similar over a rather wide σ range ($\sigma = \pi n Z^{-1/3} \leqslant 3.3$). This part of the spectrum in the given coordinates is actually common for all elements and corresponds to the filled shells of the inert gas atoms nearest to them in terms of atomic number. This fact explains the representation of the electron configuration of an element through the respective inert gas.

Accordingly, $\lg|e(\sigma)|$ interpolations for inert gases in this part of the spectrum may provide a reasonable estimate of s-electron energies for all other elements, as confirmed by Table 1, which compares experimental data [18] with the results obtained using formula (5) for eight different atoms. Cubic interpolation (7) of function $\lg|e(\sigma)|$ is used here. The estimates for the inner shells are within a 10% error.

Table 1. s-electron binding energies $|E_{n0}|$ (in electron-volts) for certain atoms. Analytical estimate (5) with function (7) and experimental data from the tables of Ref. [18].

	$_{90}$Th		$_{75}$Re		$_{60}$Nd		$_{50}$Sn	
n	(5), (7)	[18]	(5), (7)	[18]	(5), (7)	[18]	(5), (7)	[18]
1	99,529	10,9651	69,362	71,676	44,275	43,569	30,503	29,200
2	18,779	20,472	12,267	12,527	7216	7126	4639	4465
3	4778	5182	2935	2932	1583	1575	936	884.7
4	1277	1330	704	625.4	321	319.2	160	137.1
5	279	290	125	83	41	37.5		
6	39	41.4						
	$_{40}$Zr		$_{30}$Zn		$_{20}$Ca		$_{15}$P	
1	19,193	17,998	10,435	9659	4317	4038.5	2268	2145.5
2	2671	2532	1284	1196.2	434	438.4	192	189
3	476	430.3	186	139.8	41	44.3		
4	62	50.6	15	—				

3.4 Elements of the main and transition groups

Figure 4 shows deviations from the common dependence for levels with $\sigma > 3.6$, where the filling of new shells occurs. In this part of the spectrum, specific features of transition group elements are evident. Characteristically, the spectrum exhibits almost horizontal sections at which $\lg|e|$ is virtually independent of σ.

As an example, Figs 6, 7 present, together with results for inert gases, the dependences for elements of transition iron and lanthanum groups. Figures 6, 7 relate the horizontal sections in Fig. 4 to the elements of the respective group and confirm the common dependence in all the atoms. The dependence is fairly well described by the interpolating curve built for inert gases and provides a basis for energy estimation in the filled shells.

The energies of s-electrons in transition group elements can also be quantitatively estimated in the shells being filled. Strictly horizontal sections would imply that $E_{n0} = \gamma_n Z^{4/3}$, where the constant γ_n could be determined from the known value of the respective level in another element of the same group. The analysis showed, however, that this rule is not strictly followed, even if it helps to determine the range of maximum fluctuations of s-electron binding energies in a n-shell being filled from the relation

$$E_{n0}^{\max} = E_{n0}^{\min}\left[\frac{Z_{\max}}{Z_{\min}}\right]^{4/3}, \qquad (8)$$

where $Z_{\min}$ and $Z_{\max}$ are the minimal and maximum atomic numbers of the elements in a given transition group. Once two

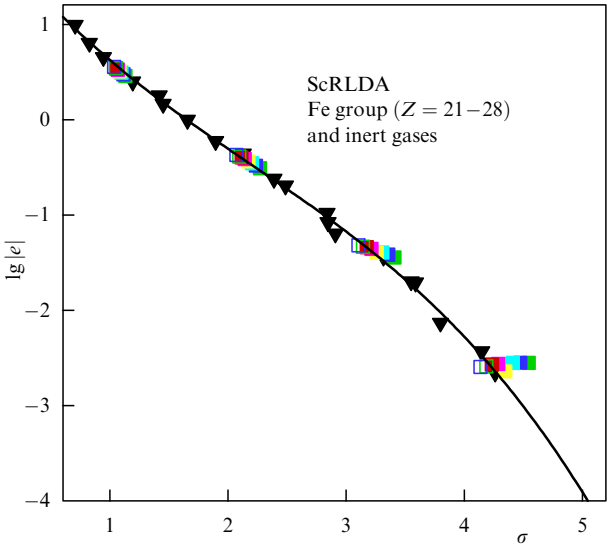

Figure 6. (Color online.) Dependence $\lg|e(\sigma)|$ for iron group elements ($Z = 21-28$) (color symbols). Graphical interpretation of the binding energies calculated by the scalar relativistic ScRLDA model [23]. Dark ▽ symbols mark inert gases. The curve is the interpolation over them.

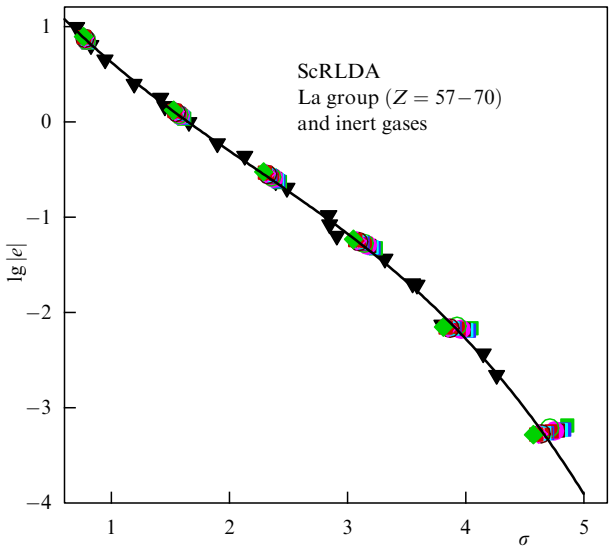

Figure 7. (Color online.) The same as in Fig. 6, for lanthanum group elements ($Z = 57-70$).

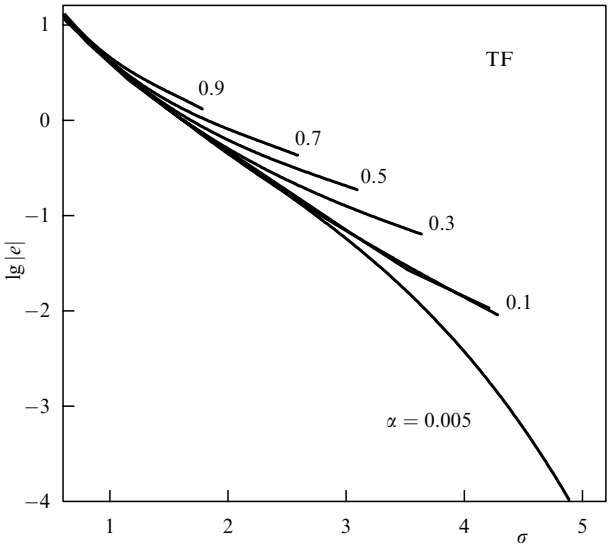

Figure 8. Function $\lg|e(\sigma,\alpha)|$ ($\alpha = z/Z$) at different ionization degrees $\alpha = 0.005, 0.1, 0.3, 0.5, 0.7, 0.9$ in the TF model.

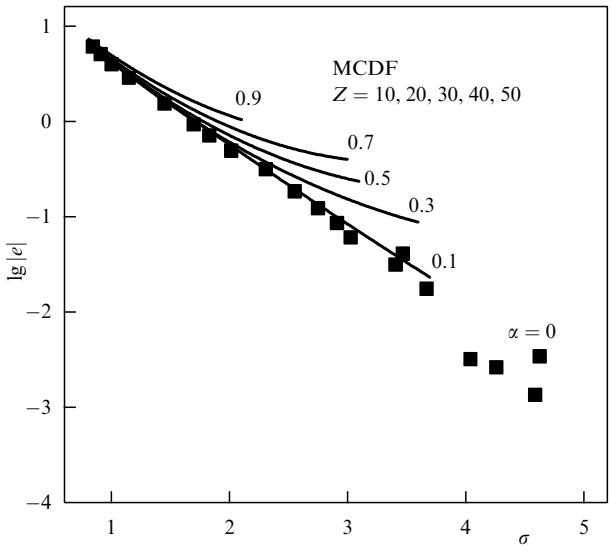

Figure 9. Functions $\lg|e(\sigma,\alpha)|$ constructed from electron binding energies E_{n0} [24] in the MCDF model [9] for ions of elements with $Z = 10, 20, 30, 40, 50$ at different ionization degrees α. Curves are the quadratic interpolations, and symbols are the values of the function $\lg|e(\sigma,0)|$ for an atom.

shells are being filled, as in the lanthanum group including rare-earth elements, relation (8) describes the range of energy variations in a shell with greater n ($n = 5$).

4. Binding energies of s-electrons in free many-electron positive ions

The analysis is based on the TF model (1), (2), as before. In the case of ions, the potential (therefore, all other ion characteristics) in this model acquires dependence on the degree of ion ionization α as a parameter; α determines the range of σ variation as well.

The same formula (6) with the function $\varphi_{\mathrm{TF}}(x;\alpha)$ yields dependences of the reduced energy $|e(\sigma;\alpha)|$ on the reduced action σ, shown in Fig. 8 for several degrees of ion ionization α.

Figures 8 and 9 make it possible to compare the dependences obtained in the TF model with the results of analysis of electron binding energies in ions from tables [24]. These tables include data for all ions of elements from hydrogen to cerium ($Z = 58$) calculated by the multiconfiguration Dirac–Fock (MCDF) model [9]. Multiple-of-ten atomic numbers are used for convenience in calculations of the degree of ionization for selected ions.

In Fig. 9 symbols denote the function $\lg|e(\sigma,0)|$ for an atom, and curves present quadratic interpolations. For simplicity, quadratic interpolations for ions are presented:

$$\lg|e(\sigma,\alpha)| = \sum_{k=0}^{2}\sum_{m=0}^{2} c_m^k \alpha^m \sigma^k\,, \qquad (9)$$

Table 2. Coefficients c_m^k in formula (9).

	c_m^k		
$m \setminus k$	0	1	2
0	1.5372	−0.9557	0.0204
1	0.6420	−1.0414	0.3944
2	−0.5089	0.8363	−0.2225

which fairly well describe results of calculations by the MCDF model. Interpolation coefficients are presented in Table 2. Figures 8 and 9 demonstrate the analogous behavior of functions $\lg|e(\sigma,\alpha)|$, which reflects clear regularities despite the quantitative difference.

5. Semiclassical analysis of the dependence of electron binding energies on the orbital angular momentum

5.1 Energy levels in the atomic potential

Atomic potentials are central potentials having a Coulomb singularity around zero. A quasiclassical analysis of binding energies in states with nonzero orbital angular momentum in systems with this potential was reported in Refs [3, 25]. The nonrelativistic energy levels E_{nl} were determined from the Bohr–Sommerfeld quantization condition (cf. condition (4) for the s-level):

$$S_E(\lambda) = \int_{R'_{E\lambda}}^{R_{E\lambda}} \sqrt{p_E^2(r) - \frac{\lambda^2}{r^2}}\,\mathrm{d}r = \pi\left(n - l - \frac{1}{2}\right) = \pi(n-\lambda)\,, \quad l > 0\,. \tag{10}$$

Here, $p_E(r) = \sqrt{2(E - U(r))}$, and $S_E(\lambda)$ stands for the radial action of an electron with energy E and orbital angular momentum $\lambda = l + 1/2$, the integration domain being bounded by turning points $R'_{E\lambda}$, $R_{E\lambda}$.

The Taylor series expansion of the quantization condition (10) in terms the orbital angular momentum λ indicates [25] that the removal of orbital degeneracy in the first approximation in λ leads to a quadratic orbital angular momentum dependence of the energy deviation from the s-level:[3]

$$E_{nl} = E_{n0} - \frac{S''_{E_{n0}}(0)}{2T_{E_{n0}}}\,\lambda^2 + \ldots, \tag{11}$$

confirmed even for $l \geqslant 1$ [3]. Here, $T_E = \partial S_E/\partial E$ is classic time, $S''_{E_{n0}}(0)$ is the second derivative of radial action $S_E(\lambda)$ with respect to λ at point $\lambda = 0$, and E_{n0} is found from formula (4).

Notice nonetheless the approximate character of quadratic formula (11) whose applicability domain is difficult to evaluate in the theoretical framework. It should also be emphasized that relations (10), (11) hold for nonrelativistic energy levels, whereas relativistic effects acquire significance in heavy atoms and ions. Specifically, spin-orbit interactions result in the splitting of energy levels with nonzero orbital angular momenta; in this case, quantum numbers n, l alone are not enough to calculate binding energies. Scalar relativistic models, e.g., ScRLDA [11] or model [13], ignore the splitting, and the influence of relativistic effects is taken into account for 'effective' energy levels E_{nl} that continue to be doubly numbered in n, l.

The nonrelativistic results are first discussed in the next section.

5.2 Energy levels with $l > 0$ in the Thomas–Fermi model

Sections 3 and 4 concerned the calculation of s-level energies E_{n0} in formula (11) in the framework of the TF model from relations (6) and the separation of function $e(\sigma)$ independent of the atomic number.

Taking account of expressions

$$T_E = Z^{-1}\tau(e)\,, \quad S''_{E_{n0}}(0) = -Z^{-1/3}\delta(e)\,, \tag{12}$$

$$\tau(e) = \frac{c^{3/2}}{\sqrt{2}}\int_0^{X_e} \frac{\mathrm{d}x}{\sqrt{\varphi(x)/x + ce}}\,, \tag{13}$$

$$\delta(e) = \frac{1}{\sqrt{2c}}\left[\int_0^{X_e}\left(\frac{1}{\sqrt{\varphi(x)/x + ce}} - \frac{1}{\sqrt{1/x + ce}}\right)\frac{\mathrm{d}x}{x^2} - 2\sqrt{\frac{1}{X_e} + ce}\right] \tag{14}$$

allows the dependence on Z and λ in the electron binding energy (11) to be separated in the explicit form

$$E_{nl} = Z^{4/3}e_n + Z^{2/3}d(e_n)\lambda^2\,, \quad d(e_n) = \frac{\delta(e_n)}{2\tau(e_n)}\,. \tag{15}$$

As a result, Eqn (15) contains one more function $d(e_n)$ independent of the atomic number Z, besides the previously considered e_n function. It proved convenient to use the respective action σ_n rather than the s-level energy e_n as the argument of this function. Taking into consideration in the general case the dependence on the degree of ionization α, this leads to two simple relations for the calculation of electron binding energies in atoms and ions via two Z-independent functions:

$$E_{nl}(Z;\alpha) = Z^{4/3}e(\sigma_n;\alpha) + Z^{2/3}d(\sigma_n;\alpha)\lambda^2\,, \quad \sigma_n = \pi n Z^{-1/3}\,, \quad \alpha = \frac{z}{Z}\,. \tag{16}$$

Function $d(\sigma)$ for atoms in the TF model is plotted in Fig. 10. Similar to function $e(\sigma)$, $d(\sigma)$ values vary in a broad range (a few orders of magnitude) upon a change in σ by several units.

As a result, the joint use of atomic number similarity in the TF model and approximation of the quadratic dependence of energy levels on the orbital angular momentum leads to atomic number and orbital angular momentum scaling of electron binding energies:

$$E_{nl} - E_{n0} \sim Z^{2/3}\lambda^2\,. \tag{17}$$

In what follows, we seek confirmation of this observation by more reliable theoretical and experimental data for atoms and ions.

6. Binding energies of electrons with nonzero orbital angular momenta in atoms

To verify the found patterns documented in experimental spectra and obtained in more sophisticated quantum-mechanical models, it is necessary to determine e_n and d_{nl} quantities from the available electron binding energies $\{E_{nl}\}$ of different elements. A method for the construction of the

[3] The next term must contain the fourth power of λ and the fourth derivative of radial action over λ at point $\lambda = 0$.

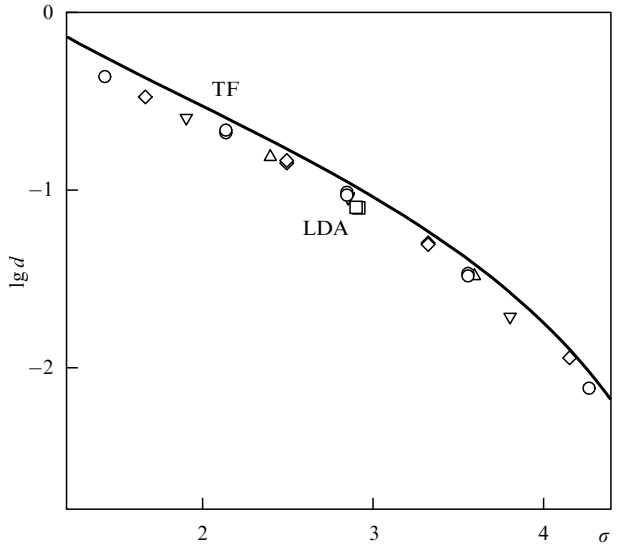

Figure 10. Function $\lg d(\sigma)$ calculated by the TF model (curve) and deduced from calculations [23] by nonrelativistic LDA model [11] for inert gas atoms (symbols: notations are the same as in Fig. 1).

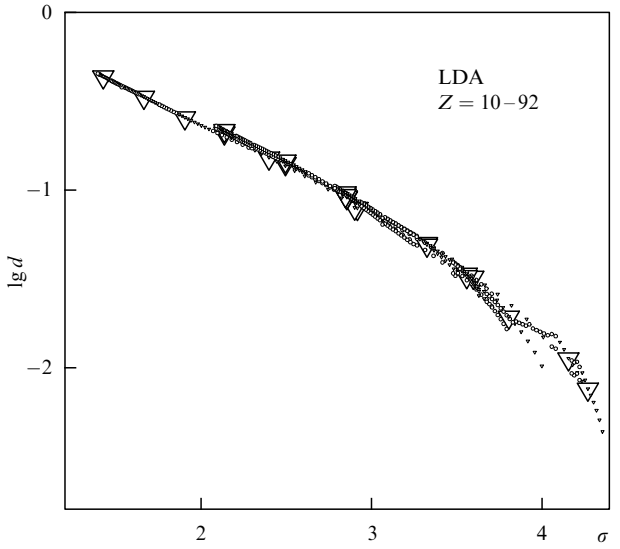

Figure 11. Function $\lg d(\sigma)$ calculated from E_{nl} levels in nonrelativistic LDA model [23] for atoms of all elements from neon to uranium: ▽ is the main group elements (large symbols ▽ mark inert gases), and ○ is the transition group elements.

dependence $e(\sigma)$ based on s-level energies E_{n0} was described in Section 3.2.

Assuming that relation (16) is valid, d_{nl} can be calculated from the available $\{E_{nl}\}$ values as a reduced deviation from the respective s-level:

$$d_{nl} = \frac{E_{nl} - E_{n0}}{Z^{2/3}\lambda^2}\,, \tag{18}$$

that is assigned the quantity $\sigma_n = \pi n/Z^{1/3}$. It is not apparent immediately that pairs $d_{nl}-\sigma_n$ for different atoms and different l and n can produce a smooth monotonic dependence and thereby confirm scaling (17).

6.1 Nonrelativistic calculations in atoms

Figure 10 presents function $d(\sigma)$ deduced from the TF model (curve) together with the results of applying equation (18) to the binding energies [23] calculated by the nonrelativistic density functional model LDA [11] for five inert gases (symbols). The figure shows the unique smooth dependence analogous to but not coincident with the TF curve.

Results of processing (18) calculations [23] by the LDA model for all atoms from neon to uranium presented in Fig. 11 demonstrate the apparent coincidence with the function for inert gases in the range of $\sigma \leqslant 3.6$. This means that scaling (17) in the spectral region is valid (within logarithmic accuracy), and the interpolation functions $\lg|e(\sigma)|$, $\lg d(\sigma)$ constructed for inert gases can be used in this region to estimate nonrelativistic energy levels in the filled shells of an arbitrary atom.

For middle atoms with atomic numbers $10 \leqslant Z \leqslant 40$, relativistic effects are insignificant; similar results are obtained using the scalar relativistic model ScRLDA (Fig. 12).

Table 3 presents interpolation coefficients for functions $\lg|e(\sigma)|$ and $\lg d(\sigma)$ calculated from the results obtained for inert gases in the ScRLDA model [23].

Table 4 compares experimental binding energies [18] for certain atoms and estimates using formula (16) with coefficients from Table 3. It follows that the filled shells are described with an error of less than 10%.

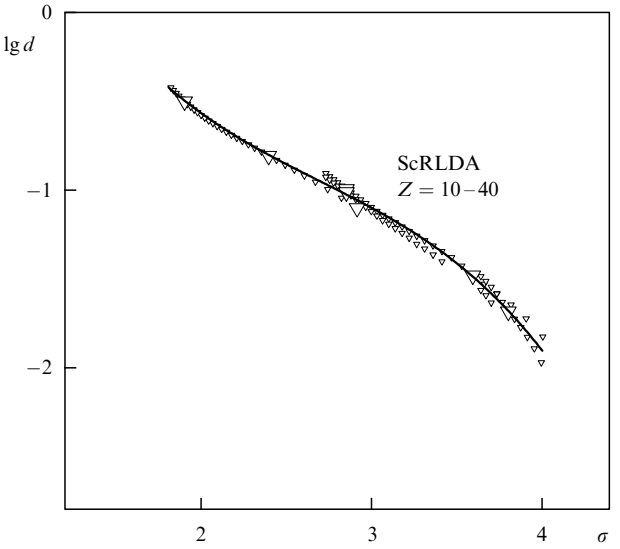

Figure 12. Function $\lg d(\sigma)$ in scalar relativistic model ScRLDA [23] for elements with atomic numbers $Z = 10-40$. Curve is the interpolation (see Table 3) over inert gases neon, argon, and krypton, denoted by large symbols ▽.

Table 3. Polynomial coefficients a_k and b_k of cubic interpolation of functions $\lg|e(\sigma)| = \sum_{k=0}^{3} a_k\sigma^k$ and $\lg d(\sigma) = \sum_{k=0}^{3} b_k\sigma^k$, respectively, based on the electron binding energies in inert gases calculated by the ScRLDA model [23].

k	a_k (Ne–Rn)	b_k (Ne–Kr)
0	1.89978	3.16641
1	−1.55642	−3.63096
2	0.32334	1.17265
3	−0.04885	−0.14540

6.2 Influence of relativistic effects

An entirely different picture is observed for heavy atoms. Figure 13 demonstrates the dependence of $\lg d_{nl}$ on σ for all elements from neon to uranium obtained from ScRLDA

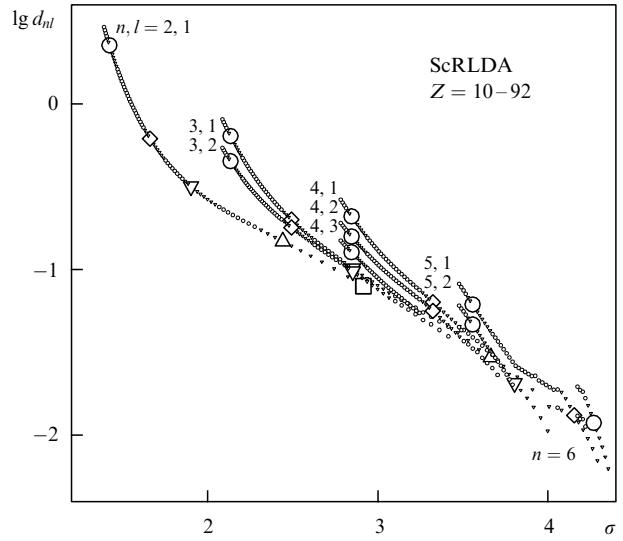

Figure 13. Function $\lg d_{nl}(\sigma)$ in the scalar relativistic model ScRLDA [23] for atoms of all elements from neon to uranium. Small symbols ▽ and ○ mark the elements of main and transition groups, respectively. Large symbols denote inert gases: neon — □, argon — △, krypton — ▽, xenon — ◇, and radon — ○. Numbers — n, l values.

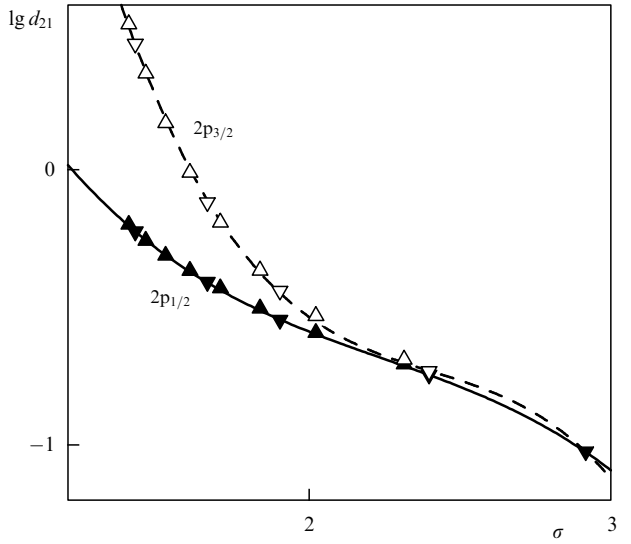

Figure 14. Function $\lg d_{21}(\sigma)$ for inert gases (▽) and elements with atomic numbers $Z = 20$, 30, 40, 50, 60, 70, 80, 90 (△). Filled symbols mark the $2p_{1/2}$ states; unfilled symbols are the $2p_{3/2}$ states. Curves are the interpolating cubic polynomials for inert gases. Processing of experimental data [18].

Table 4. Experimental electron binding energies in certain atoms [18] compared with estimates using formula (16) with coefficients from Table 3 (in atomic units).

		Cl ($Z = 17$)		K ($Z = 19$)		Cu ($Z = 29$)	
n	l	$-\varepsilon_{nl}$ [18]	$-\varepsilon_{nl}$ (16)	$-\varepsilon_{nl}$ [18]	$-\varepsilon_{nl}$ (16)	$-\varepsilon_{nl}$ [18]	$-\varepsilon_{nl}$ (16)
1	0	104	108	133	138	330	350
2	0	9.92	9.02	13.91	12.40	40.3	39.9
2	1	7.39	6.80	10.90	9.83	34.6	34.6
3	0					4.5	5.1
3	1					2.8	3.5
		Zn ($Z = 30$)		Br ($Z = 35$)		Zr ($Z = 40$)	
1	0	355	376	527	523	661	694
2	0	44	43.7	70.6	65.4	93.1	92.2
2	1	38	38	62.6	58	83.2	82.8
3	0	5.14	5.76	10.8	9.77	15.8	15.1
3	1	3.31	4.10	8.02	7.57	12.4	12.4
3	2	0.37	1.13	3.47	3.65	6.62	7.43
4	0			1.01	0.96	1.86	1.82
4	1			0.52	0.50	1.02	1.08

'effective' levels. Separate filled (n, l) shells exhibit smooth $\lg d_{nl}(\sigma)$ dependences, but they fail to form, even approximately, a common functional dependence, as in the nonrelativistic LDA model (see Fig. 11) or in the same ScRLDA model for middle atoms (see Fig. 12).

Nevertheless, it turns out that $\lg d_{nl}(\sigma)$ dependences can also be represented through interpolation of relevant values for each filled shell in inert gases, even with regard for level splitting due to spin-orbit interaction. Such an example for experimental energies $E_{2p_{1/2}}$ and $E_{2p_{3/2}}$ is shown in Fig. 14 presenting results for more eight atoms from calcium to thorium, besides those for inert gases. Thus, smooth dependences are confirmed for split levels too, and the complete picture of $\lg d_{nl}(\sigma)$ is extended, in comparison with Fig. 13, by one more ramification of each branch analogous to that depicted in Fig. 14.

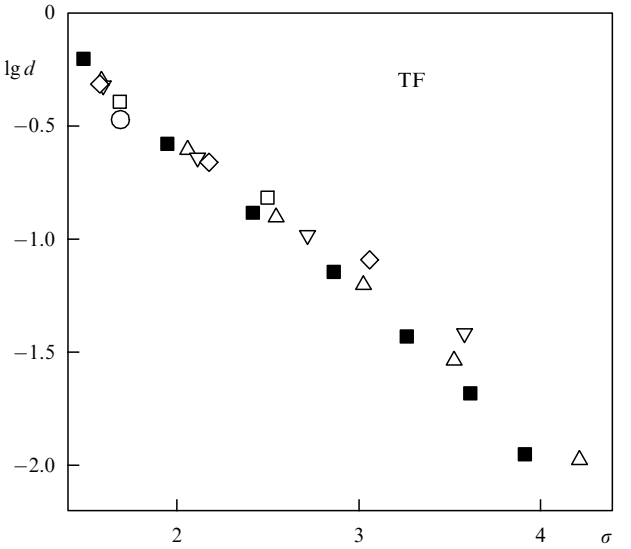

Figure 15. Function $d(\sigma, \alpha)$ from the TF model for different degrees of ionization: $\alpha = 0.005$ — ■, 0.1 — △, 0.3 — ▽, 0.5 — ◇, 0.7 — □, and 0.9 — ○.

7. Binding energies of electrons with nonzero orbital angular momenta in ions

7.1 Ions of elements with atomic numbers $Z < 58$

In this section, the same dependences are discussed for ions, with one more parameter (degree of ionization α) being included in the consideration.

Figure 15, presenting function $\lg d(\sigma, \alpha)$ for different degrees of ionization in the TF model, demonstrates its relatively weak dependence on the degree of ionization, especially for the inner filled shells ($\sigma < 3$). In other words, parameter α in the TF model, having a strong influence on the range of σ variation (that naturally narrows with growing the

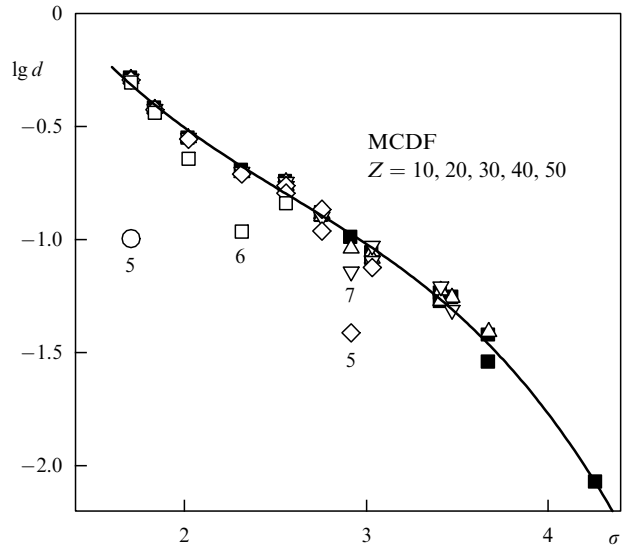

Figure 16. Function $d(\sigma, \alpha)$ constructed from electron energy levels E_{nl} [24] in the MCDF model [9] for elements with atomic numbers $Z = 10$, 20, 30, 40, 50 at different α: $\alpha = 0$ — ■; other notations are as in Fig. 15. Cipher under a symbol denotes the number of electrons in an ion. Curve plots the cubic interpolation over many-electron ions.

Table 5. Electron binding energies (in electron-volts) in certain ions of different elements from tables [24] calculated in the MCDF model [9] and analytical estimation using formula (16) with functions (9), and (19).

	$_{58}Ce^{+4}$		$_{56}Ba^{+7}$		$_{55}Cs^{+12}$		$_{54}Xe^{+24}$	
nl	$\lvert E_{nl}\rvert$ [24]	$\lvert E_{nl}\rvert$ (16)	$\lvert E_{nl}\rvert$ [24]	$\lvert E_{nl}\rvert$ (16)	$\lvert E_{nl}\rvert$ [24]	$\lvert E_{nl}\rvert$ (16)	$\lvert E_{nl}\rvert$ [24]	$\lvert E_{nl}\rvert$ (16)
1s	40,499	36,723	37,543	34,581	36,229	33,832	35,352	33,856
2s	6614	6701	6097	6192	5963	6042	6226	6343
2p	5782	6190	5349	5708	5254	5573	5556	5888
3s	1501	1408	1396	1362	1456	1459	1870	1926
3p	1247	1240	1166	1202	1236	1304	1660	1776
3d	944	940	881	919	959	1029	1400	1508
4s	357	341	361	368	454	476	818	947
4p	275	277	286	309	375	419		
4d	165	164	186	205	289	319		
5s	89	95	113	122				
5p	65	81	100	110				
	$_{42}Mo^{+20}$		$_{34}Se^{+14}$		$_{20}Ca^{+3}$		$_{30}Zn^{+18}$	
1s	20,756	20,646	13,138	13,281	4087	4228	10,405	10,730
2s	3607	3637	2137	2125	488	458	1908	1903
2p	3259	3332	1912	1906	393	362	1733	1724
3s	1131	1160	632	637	89	78	693	777
3p	1012	1061	552	568	66	56		
3d	890	884	473	446				

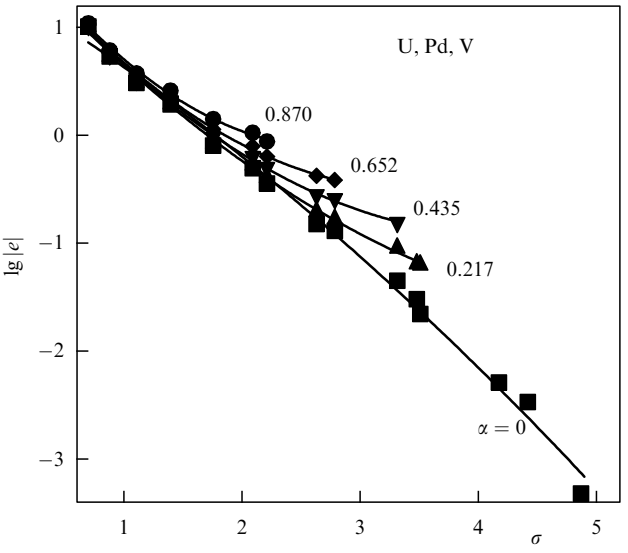

Figure 17. Function $\lg |e(\sigma, \alpha)|$ constructed from electron energy levels E_{n0} from Ref. [24] (for $Z = 23$, $Z = 46$) and Ref. [10] (for $Z = 92$) at different degrees of ionization α denoted by different symbols.

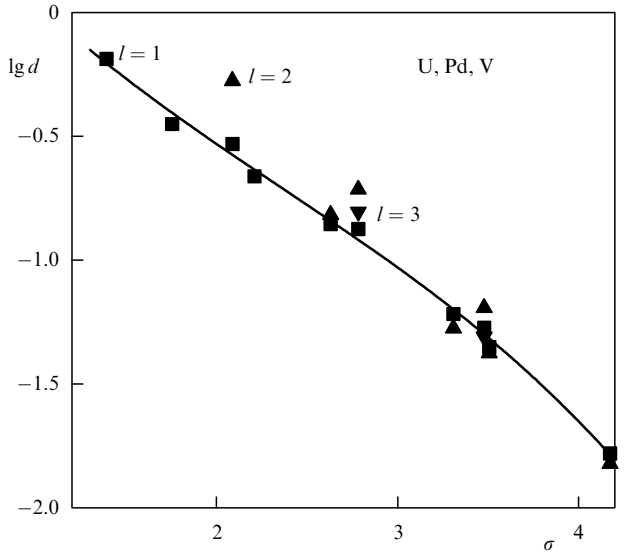

Figure 18. Function $\lg d(\sigma, \alpha)$ constructed from electron energy levels $E_{nl,\,j=l-1/2}$ [24] (for $Z = 23$, $Z = 46$) and [10] (for $Z = 92$) and independent of the degree of ionization. Identical symbols denote identical values of orbital angular momentum l: ■ — $l = 1$, ▲ — $l = 2$, and ▼ — $l = 3$.

degree of ionization), only weakly affects the behavior of function $\lg d(\sigma, \alpha)$ within this range.

The $d(\sigma, \alpha)$ dependence calculated in the more advanced quantum-mechanical model MCDF [9] was reconstructed from ionization energy levels E_{nl} in tables [24] using the same algorithm (18). Results of this treatment are presented in Fig. 16, confirming the weak dependence of function $d(\sigma, \alpha)$ on α for many-electron ions in the TF model. Indeed, all deviations from this general dependence in Fig. 16 are due to a small number of electrons in the ion ($N_e < 10$).

This means that, in this case too, the available data can be described using the α-independent function $d(\sigma)$. The curve in Fig. 16 is the interpolation of this function using the cubic polynomial

$$\lg d(\sigma; \alpha) \cong \lg d(\sigma) = \sum_{k=0}^{3} b_k \sigma^k , \qquad (19)$$

with coefficients b_k equaling $b_0 = 2.1117$, $b_1 = -2.4106$, $b_2 = 0.7424$, and $b_3 = -0.0956$.

The above analysis shows the possibility of employing the α-independent function $d(\sigma)$ provided the following conditions are fulfilled:

(1) the atomic number $Z \geqslant 10$,

(2) the number of electrons in an ion $N_e \geqslant 10$.

These conditions are compatible with the applicability domain of the TF model, the use of which 'prompted' the above atomic number and degree of ionization scalings.

Interpolations (9), (19) of functions $e(\sigma,\alpha)$, $d(\sigma)$ are used to compare analytical estimates using formula (16) and the results of exact calculations of electron binding energies [24] in the MCDF model [9] for certain ions of different elements. The interpolations are constructed based on data [24] for ions of five elements with $Z = 10, 20, 30, 40, 50$. The test elements and ions were selected so as to fully represent different variants. The results for eight ions are collected in Table 5. In this case too, the estimates for the filled shells are within 10% error.

7.2 Heavy elements

Results of the scaling can be of practical interest for the estimation of electron binding energies in inner shells of heavy element ions for which published data are absent. They are needed for experimental studies and the calculation of the ionization cross sections of many-electron atoms and ions by electrons and heavy particles with a great contribution from inner shell electrons. Therefore, the present section was designed to generalize this method to heavy elements too, even though it does not allow taking into account relativistic effects (level splitting due to spin-orbit interactions).

To begin with, interpolations of functions $\lg|e(\sigma;\alpha)|$, $\lg d(\sigma;\alpha)$ used in Section 7.1 to calculate tables of middle

Table 6. Coefficients c_m^k in formula (20).

	c_m^k			
$m \setminus k$	0	1	2	3
0	1.9347	-1.5763	3.2347×10^{-1}	-4.4599×10^{-2}
1	4.4638×10^{-2}	-1.2033×10^{-1}	8.8302×10^{-2}	-6.8499×10^{-3}
2	-5.1722×10^{-1}	1.5664	-1.4676	4.4901×10^{-1}
3	1.2590	-3.3788	2.9163	-7.7141×10^{-1}
b_k	8.7553×10^{-1}	-1.0343	2.3039×10^{-1}	-3.2415×10^{-2}

Table 7. Electron binding energies $|E_{nlj}|$ (in electron-volts) in certain uranium ions from Table 10 calculated based on the MCDF model [9] and analytical estimation by formula (16) with functions (20) (index * stands for $j = l - 1/2$; in the absence of an index, $j = l + 1/2$).

	U^{+10}		U^{+20}		U^{+30}		U^{+40}	
nl	$\lvert E_{nl}\rvert$ [10]	$\lvert E_{nl}\rvert$ (16)	$\lvert E_{nl}\rvert$ [10]	$\lvert E_{nl}\rvert$ (16)	$\lvert E_{nl}\rvert$ [10]	$\lvert E_{nl}\rvert$ (16)	$\lvert E_{nl}\rvert$ [10]	$\lvert E_{nl}\rvert$ (16)
1s	1.166×10^5	1.079×10^5	1.169×10^5	1.082×10^5	1.173×10^5	1.088×10^5	1.180×10^5	1.098×10^5
2s	2.208×10^4	2.014×10^4	2.237×10^4	2.040×10^4	2.280×10^4	2.078×10^4	2.352×10^4	2.135×10^4
2p*	2.127×10^4	1.936×10^4	2.156×10^4	1.962×10^4	2.199×10^4	2.000×10^4	2.271×10^4	2.057×10^4
2p	1.744×10^4		1.773×10^4		1.816×10^4		1.888×10^4	
3s	5.768×10^3	5.233×10^3	6.052×10^3	5.573×10^3	6.459×10^3	6.058×10^3	7.176×10^3	6.708×10^3
3p*	5.400×10^3	4.901×10^3	5.685×10^3	5.241×10^3	6.093×10^3	5.726×10^3	6.815×10^3	6.376×10^3
3p	4.508×10^3		4.791×10^3		5.198×10^3		5.907×10^3	
3d*	3.928×10^3	4.310×10^3	4.214×10^3	4.650×10^3	4.623×10^3	5.135×10^3	5.348×10^3	5.785×10^3
3d	3.748×10^3		4.032×10^3		4.442×10^3		5.151×10^3	
4s	1.622×10^3	1.563×10^3	1.898×10^3	1.894×10^3	2.285×10^3	2.389×10^3	2.908×10^3	3.016×10^3
4p*	1.456×10^3	1.412×10^3	1.732×10^3	1.744×10^3	2.117×10^3	2.238×10^3	2.748×10^3	2.865×10^3
4p	1.220×10^3		1.494×10^3		1.877×10^3		2.476×10^3	
4d*	9.532×10^2	1.144×10^3	1.229×10^3	1.475×10^3	1.611×10^3	1.970×10^3	2.226×10^3	2.597×10^3
4d	9.094×10^2		1.182×10^3		1.566×10^3		2.154×10^3	
4f*	5.576×10^2	7.417×10^2	8.331×10^2	1.073×10^3	1.218×10^3	1.568×10^3	1.849×10^3	2.194×10^3
4f	5.463×10^2		8.206×10^2		1.206×10^3			
5s	4.839×10^2	4.434×10^2	7.352×10^2	6.876×10^2	1.053×10^3	1.130×10^3		
5p*	4.167×10^2	3.808×10^2	6.696×10^2	6.250×10^2				
5p	3.595×10^2		5.978×10^2					
5d*	2.561×10^2	2.695×10^2	4.981×10^2	5.137×10^2				
5d	2.469×10^2							
5f	—	1.025×10^2						
6s	1.799×10^2	9.866×10^1						
6p*	1.576×10^2	7.824×10^1						
	U^{+50}		U^{+60}		U^{+70}		U^{+80}	
1s	1.190×10^5	1.114×10^5	1.200×10^5	1.137×10^5	1.219×10^5	1.169×10^5	1.245×10^5	1.212×10^5
2s	2.444×10^4	2.217×10^4	2.550×10^4	2.332×10^4	2.724×10^4	2.490×10^4	2.952×10^4	2.704×10^4
2p*	2.363×10^4	2.139×10^4	2.470×10^4	2.254×10^4	2.649×10^4	2.412×10^4	2.880×10^4	2.627×10^4
2p	1.980×10^4		2.085×10^4		2.258×10^4		2.486×10^4	
3s	8.060×10^3	7.553×10^3	9.000×10^3	8.632×10^3	1.038×10^4	9.994×10^3	1.201×10^4	1.170×10^4
3p*	7.700×10^3	7.220×10^3	8.652×10^3	8.299×10^3	1.009×10^4	9.661×10^3		
3p	6.785×10^3		7.712×10^3		9.051×10^3			
3d*	6.229×10^3	6.630×10^3	7.181×10^3	7.708×10^3	8.661×10^3	9.071×10^3		
3d	6.038×10^3		6.989×10^3					
4s	3.634×10^3	3.665×10^3	4.370×10^3	4.124×10^3				
4p*	3.476×10^3	3.514×10^3	4.222×10^3	3.973×10^3				
4p	3.170×10^3							
4d*	2.928×10^3	3.246×10^3						
4d	2.867×10^3							

elements give but an inadequate description of binding energies in uranium ions, as confirmed by comparison with the results of calculations in the Dirac–Fock model [10]. To extend the applicability region for our approach to a broader range of atomic numbers, we built up new interpolations for these functions with the use of data on orbital binding energies in atoms and ions of three elements with $Z = 23, 46, 92$.

Figures 17 and 18 present the results of processing these data. To construct function $\lg d(\sigma;\alpha)$, the energy of the level with $j = l - 1/2$ was chosen from two split energy levels E_{nlj} with $l > 0$. In Fig. 17, the data for different elements are arranged into groups with identical degrees of ionization denoted by different symbols. Figure 18 illustrates independence of function $\lg d_l(\sigma;\alpha)$ from the degree of ionization. Most data can be interpolated by a single curve, shown in Fig. 18. However, for heavy uranium, an uncommon dependence on orbital angular momentum l emerges. All appreciable deviations from the general curve correspond to the energies in uranium ions with $l = 2, 3$. At the same time, much larger deviations occur if the energies E_{nlj} with $j = l + 1/2$ are involved. Obviously, this limits the accuracy of our estimates of orbital energies with $l > 1$ in heavy elements, as confirmed by the comparison for uranium (see Table 7).

The common dependences in Figs 17 and 18 are interpolated using cubic polynomials:

$$\lg\left|e(\sigma,\alpha)\right| = \sum_{k=0}^{3}\sum_{m=0}^{3} c_m^k \alpha^m \sigma^k\,, \quad \lg d(\sigma) = \sum_{k=0}^{3} b_k \sigma^k\,, \quad (20)$$

with coefficients c_m^k and b_k from Table 6. Table 7 collates the orbital energies from Ref. [10] and results of our analytical estimations using formula (16) with functions $e(\sigma,\alpha)$, $d(\sigma,\alpha)$ in accordance with formulas (20). Evidently, only an estimate of 4d and 4f levels for the inner filled shells results in poorer accuracy. In the other cases, the estimated error does not exceed 10%.

Calculations show that the extended interpolation (20) for middle-atomic-number elements is slightly worse than the one more oriented to such elements with functions (9), (19). Interpolation (20) overestimates the energy values but also results in an error below 10% for the filled shell levels.

8. Conclusions

We examined properties of the intraatomic potential and orbital binding energies in many-electron atoms and ions based on the analysis of a large body of available empirical data and calculations in the framework of quantum-mechanical models. The general view of the relationship between these characteristics and the atomic number of an element and the degree of ionization of its ion confirms the dependences on them deduced from the TF model, albeit with different functional coefficients. Simple interpolations of these functions-coefficients make it possible to construct an approximate radius dependence of intraatomic potential in the central part of an atom and analytically estimate electron binding energies in the inner filled shells of a many-electron atom or ion using a small number of tabulated constants.

Certainly, the scaling revealed in experimental data and quantum-mechanical calculations is an approximate one. The general patterns visible in the figures are represented on the semilogarithmic scale, which precludes a spectroscopic accuracy of estimation. It is shown that results for the inner filled shells are within 10% and 10–30% of the exact evaluation for middle and heavy elements, respectively. These estimates are not very accurate but can be used as an initial approximation in precise computations and also for the rough calculation of the ionization cross sections of many-electron atoms and ions by electrons and heavy particles, when failing more precise data.

Moreover, separating functions $e(\sigma,\alpha)$, $d(\sigma)$ allows compactly presenting copious information on all binding energies in any number of many-electron elements, revealing peculiarities of shell filling in the main and transition groups, and evaluating the role of relativistic effects. These possibilities may be used for educational purposes. A recent publication [26] shows that the application of Z-scaling for the analysis of X-ray terms makes it possible to describe experimental data with an error of less than 1% and monitor measurement reliability.

Acknowledgments

The author is deeply grateful to A S Grushin and P R Levashov for procuring results of calculations of intraatomic potentials in inert gas atoms from the Hartree–Fock–Slater (HFS) model [12] and by the density functional method [13], respectively.

References

1. Landau L D, Lifshitz E M *Quantum Mechanics. Non-Relativistic Theory* (Oxford: Pergamon Press, 1977); Translated from Russian: *Kvantovaya Mekhanika. Nerelyativistskaya Teoriya* (Moscow: Fizmatlit, 1989)
2. Kirzhnits D A, Lozovik Yu E, Shpatakovskaya G V *Sov. Phys. Usp.* **18** 649 (1975); *Usp. Fiz. Nauk* **117** 3 (1975)
3. Shpatakovskaya G V *Phys. Usp.* **55** 429 (2012); *Usp. Fiz. Nauk* **182** 457 (2012)
4. Dyachkov S A, Levashov P R *Phys. Plasmas* **21** 052702 (2014)
5. Gombás P *Die statistische Theorie des Atoms und ihre Anwendungen* (Wein: Springer-Verlag, 1949); Translated into Russian: *Statisticheskaya Teoriya Atoma i Ee Primeneniya* (Moscow: IL, 1951)
6. Shevelko V P, Vinogradov A V *Phys. Scripta* **19** 275 (1979)
7. Vinogradov A V, Tolstikhin O I *Sov. Phys. JETP* **69** 683 (1989); *Zh. Eksp. Teor. Fiz.* **96** 1204 (1989)
8. Sigmund P *Particle Penetration and Radiation Effects* Vol. 2 (Springer Series in Solid-State Sciences, Vol. 179) (Berlin: Springer, 2014)
9. Desclaux J P *Comput. Phys. Commun.* **9** 31 (1975)
10. Rashid Kh, Saadi M Z, Yasin M *Atom. Data. Nucl. Data Tabl.* **40** 365 (1988)
11. Kotochigova S et al. *Phys. Rev. A* **55** 191 (1997)
12. Nikiforov A F, Novikov V G, Uvarov V B *Quantum-Statistical Models of Hot Dense Matter* (Basel: Birkhäuser Verlag, 2005); Translated from Russian: *Kvantovo-statisticheskie Modeli Vysokotemperaturnoi Plazmy* (Moscow: Fizmatlit, 2000)
13. Giannozzi P et al. *J. Phys. Condens. Matter* **21** 395502 (2009)
14. Kozlov M G et al. *Comput. Phys. Commun.* **195** 199 (2015)
15. Shpatakovskaya G V, Karpov V Ya *J. Phys. Conf. Ser.* **774** 012002 (2016)
16. Karpov V Ya, Shpatakovskaya G V *JETP* **124** 369 (2017); *Zh. Eksp. Teor. Fiz.* **151** 435 (2017)
17. Shpatakovskaya G V, Preprint No. 184 (Moscow: Keldysh Institute of Applied Mathematics, 2018) http://doi.org/10.20948/prepr-2018-184-e
18. X-Ray Data Booklet, Center for X-ray Optics and Advanced Light Source. Lawrence Berkeley National Laboratory, Update October 2009, http://xdb.lbl.gov/
19. Moore C E "Atomic Energy Levels", NBS Circular 467 Vol. 1 (Washington, DC: Department of Commerce, 1949); NBS Circular 467 Vol. 2 (Washington, DC: Department of Commerce, 1952); NBS Circular 467 Vol. 3 (Washington, DC: Department of Commerce, 1958)

20. Bearden J A, Burr A F *Rev. Mod. Phys.* **39** 125 (1967)
21. Cardona M, Ley L (Eds) *Photoemission in Solids* Vol. 1 *General Principles* (Berlin: Springer-Verlag, 1978)
22. Fuggle J C, Mårtensson N *J. Electron Spectrosc. Relat. Phenom.* **21** 275 (1980)
23. Atomic Reference Data for Electronic Structure Calculations. NIST Standard Reference Database 141, http://www.nist.gov/pml/data/dftdata/index.cfm; https://dx.doi.org/10.18434/T4ZP4F
24. The DREEBIT Ionization Energy Database, http://www.dreebit-ibt.com/ionization-energy-database.html
25. Shpatakovskaya G V *JETP Lett.* **73** 268 (2001); *Pis'ma Zh. Eksp. Teor. Fiz.* **73** 306 (2001)
26. Shpatakovskaya G V *JETP Lett.* **108** 768 (2018); *Pis'ma Zh. Eksp. Teor. Fiz.* **108** 781 (2018)